

2013

Ultrastructure of the Gill Rakers in American Shad, *Alosa sapidissima* (Clupeidae)

Katherine Ericson Nolan
College of William and Mary

Follow this and additional works at: <https://scholarworks.wm.edu/honorsthesis>

Recommended Citation

Nolan, Katherine Ericson, "Ultrastructure of the Gill Rakers in American Shad, *Alosa sapidissima* (Clupeidae)" (2013). *Undergraduate Honors Theses*. Paper 633.
<https://scholarworks.wm.edu/honorsthesis/633>

This Honors Thesis is brought to you for free and open access by the Theses, Dissertations, & Master Projects at W&M ScholarWorks. It has been accepted for inclusion in Undergraduate Honors Theses by an authorized administrator of W&M ScholarWorks. For more information, please contact scholarworks@wm.edu.

**Ultrastructure of the Gill Rakers in American Shad,
Alosa sapidissima (Clupeidae)**

A thesis submitted in partial fulfillment of the requirement
for the degree of Bachelors of Science in Biology from
The College of William and Mary

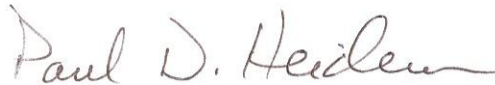
By

Katherine Ericson Nolan

Accepted for Honors



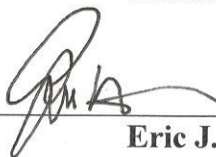
S. Laurie Sanderson, Director



Paul D. Heideman



Matthias Leu



Eric J. Hilton

Williamsburg, VA
April 29th, 2013

Abstract

The American shad (*Alosa sapidissima*) is an anadromous fish that uses suspension feeding to obtain nutrients. The oral morphology of this species is scarcely understood or documented in scientific literature. Information on the specific cell types and structure of gill rakers on the gill arches could provide significant insight into the crossflow filtration mechanism of this species. Scanning electron microscopy (SEM) and literature comparison were used to identify cell types and microstructures of the raker. Using this comparison, mucous cells, pavement cells, and chloride cells were identified. Distinct patterning and density of mucous cells and pavement cells were measured using SEM imaging and ImageJ software. A significant cell density difference was identified in mucous cells medial and lateral to the denticle structures. These data provide insight into the function of these cell types in particle filtration, water flow, organismal defense, and pH regulation.

Introduction

The American shad is a suspension-feeding fish in the family Clupeidae. This anadromous fish natively inhabits oceans off the coast of the eastern United States, but returns to freshwater habitats to spawn each season. The juvenile American shad feed mainly on zooplankton and insects while the adults mainly consume phytoplankton, small crustaceans and fishes (Bigelow et al., 2002). Preliminary investigations on the oral cavity morphology of the adult American shad suggested that crossflow filtration may be the primary particle retention method used during suspension feeding in this species (Storm, 2009). In crossflow filtration, water and miniscule food particles enter the oral cavity. As water passes between the gill arches and exits via the operculum, particle

concentration in the oral cavity increases as food flows to the back of the mouth towards the esophagus (Sanderson et al., 2001). The gill raker structures of suspension-feeding fishes were once thought to serve as a dead-end sieve through which food particles are filtered. It is now thought that instead, these structures have virtually no contact with the particles. The gill rakers appear to serve as a filter framework positioned parallel to the water as it flows into the oral cavity (Brainerd, 2001). The mechanism by which these fishes filter particles is without the use of dead-end sieving but instead through the use of crossflow filtration, which has led to an increased interest in the investigation of the morphological features of the oral cavity and their potential roles in this filtering process. If these gill raker structures are not in direct contact with food particles, what is their function? Could investigation into the raker cell types and microstructures provide insight into the role of the rakers in this species? The goal of this investigation is to provide data that can help answer these questions.

Currently, the specific role of the gill rakers in American shad is unclear. Existing literature on oral morphology is primarily focused on the gill filaments. Gill raker structures are mentioned only briefly in the literature of distantly related fish species including tilapia (*O. mossambicus*) and salmon species (Wilson and Laurent, 2002). Few investigations (Hamman, 1985) have focused specifically on the gill raker structures of American shad. Documentation of the specific microstructures and cell types on the gill rakers is virtually absent from the existing literature of fish species in general. An in-depth scanning electron microscopy (SEM) investigation into specific cell types and structures of the gill rakers on the anterior four gill arches of the American shad was used to uncover possible roles of the gill raker in feeding and filtration. Cell types including

mucous cells, pavement cells, and chloride cells as well as distinct structures known as denticles on American shad specimens were identified. Cells were identified by comparison with SEM images from primary literature sources and preliminary findings of T.J. Storm's Honors thesis research (2009).

The goal of this study was to identify distinct cell types expected to be present on the gill rakers including mucous cells and pavement cells. Chloride cells were not expected to be found on the gill raker based on existing literature on gill filaments (Zydlewski and McCormick, 1997). However, SEM images collected in this study were compared closely with SEM images in published literature to conduct a comprehensive study of gill raker cell types. Preliminary research (Fall 2011 and Spring 2102) on both mucous cells and pavement cells detected a distinct difference in the number of these cells clustered in specific regions medial and lateral to the denticle. This study investigated the significance of this distinct cell density difference at specific locations medial and lateral to the denticle on the four anterior arches in five American shad specimens. Identifying a mucous cell or pavement cell density gradient on the gill raker could provide insight into the function of these cells in the context of water flow, particle filtration, or other key roles such as tissue protection and pH regulation. Mucous cell quantification and pavement cell observations were focused in the vicinity of the denticle structures. However, denticles were also imaged for the purpose of documenting these structures, which have been described in one previous study only (Storm, 2009).

American shad are vital for the ecological and economic roles they serve. This species maintains a wide distribution along the Atlantic east coast from Canada to Florida and has been documented as a key food source in this region since pre-colonial America.

In the 17th century, population levels were extremely high and provided an abundant food source. Overfishing, pollution, habitat destruction, and climate change have brought population levels to an all-time low in the 21st century (ASMFC, 1999). Populations that were once a key link in the seasonal fishing industry in the late 18th century across the Maryland, Virginia, and Pennsylvania area were destroyed and in desperate need of reestablishment (Latour et al., 2012). Massive restoration projects have recently been underway to reinstate this integral species to historical levels, recognizing the importance of this fish. American shad are also an important member of the food web, serving as a key food source for larger predators, including the largemouth and striped bass (Stangl, 2012). In addition to the important ecological roles of the American shad, a deeper understanding of the functional roles of gill rakers in crossflow filtration holds promising possibilities for practical application to industrial filtration methods. It is undeniable that the American shad serve many key roles in the ecosystem and in human utilization, proving the merit of a deeper understanding of this species.

Methods

Specimen collection and preparation for SEM

Adult American shad specimens (Table 1) were obtained on April 16, 2012 from the Pamunkey River (37.55°N/77.03°W) with the help of Tom Gunter from Aquatic Biological Monitoring Services and Mike Isel from the Virginia Department of Game and Inland Fisheries (VDGIF). Permission was granted by Eric Brittle (VDGIF) for these individuals to provide specimens that were collected for the VDGIF restocking project. Specimens were collected using gill nets, purged of eggs or sperm, and then placed on ice to ensure preservation of oral tissue during transport. Two specimens were prepared fresh

for SEM and the remaining two were frozen for future use. Table 2 provides information for the additional three fresh specimens that were prepared by TJ Storm (2009) and used in this study.

Table 1- ID number, sex, and length measurements for Spring 2012 specimens

ID Number	Sex	Total Length	Fork Length	Standard Length
I	Female	46.0 cm	41.5 cm	39.0 cm
II	Female	44.0 cm	41.2 cm	38.5 cm

Table 2- Specimens prepared by TJ Storm in 2009 and used for this study

ID Number	Total Length	Fork Length	Standard Length
IV	48.0 cm	43.0 cm	38.5 cm
VI	49.0 cm	43.5 cm	41.0 cm
VII	43.5 cm	40.0 cm	37.5 cm

Specimen Preparation

Specimens I and II were dissected within four hours of collection to reduce tissue decay. The left operculum was removed and the arrangement of the gill arches was observed in their natural configuration (Figure 1). Fine dissection scissors and tweezers were used to remove each of the anterior four gill arches and only the gill filaments were handled with dissection tools. After each arch was removed, it was thoroughly rinsed with tap water to remove remaining mucous and blood. During the preparation of each individual arch, the remainder of the specimen was covered with a damp paper towel and stored at 4° C. Figure 2 shows the four arches and pre-esophageal tissue of Specimen II after dissection.

Each gill arch was cut into sections using a razor blade and fine dissection scissors. Sections were cut on dental wax and damp paper towels to reduce tearing and other tissue damage. Similar to procedures described by Storm (2009), gill filaments were cut shorter on the dorsal side to provide a reference under the SEM. Since the pre-

esophageal sections removed from the specimens did not have filaments, tissue on the dorsal side was cut shorter for reference.

Gill arch sections were prepared using the procedure followed by Storm (2009). Individual glass vials were labeled in advance and filled with 2.5% gluteraldehyde in 0.1M phosphate buffer (pH 7.2-7.4) and sections were fixed in these vials once cut. Gill sections were kept in gluteraldehyde solution at room temperature for 30 minutes, then placed in the refrigerator at 4° C for two hours. Gluteraldehyde solution was pipetted out of the vials and 0.1M phosphate buffer was added. Gill sections were stored in buffer solution overnight. Next, they were rinsed for two hours in 0.1M phosphate buffer and this process was repeated three times. The specimens were then placed in 16% glycerol/water solution for 24 hours. Sections were placed in a series of ethanol solutions including 20% ethanol for one hour, 50% ethanol for one hour, and then stored in 70% ethanol at 4° C overnight. Next, samples were bathed in 90% ethanol for one hour, 100% ethanol for one hour and finally stored in 100% ethanol at 4° C for 48 hours.

To prepare the specimens for mounting onto SEM stubs, each section was placed in the chemical drying agent Hexamethyldisilazane (HDMS) for five minutes. While still damp, sections were mounted onto metal stubs using standard SEM adhesive and liquid carbon adhesive. Finally, specimens were coated with a layer of gold-palladium using the Hummer Vii sputtering system. Sputtering was done at seven nm/min for eight minutes and then specimens were stored in a desiccation chamber until use. Specimens were sketched as they appeared on the SEM stub for reference (Figures 3-7).

Imaging procedure

A systematic imaging procedure was devised to ensure consistent images were taken at specific locations on the gill raker (Figure 8A). Images were taken that would provide suitable comparison of locations medial and lateral to denticles on the raker to compare mucous cell and pavement cell densities. For each of the five specimens, there were four gill arches. For each arch, a single raker was examined. Gill rakers possess a dorsal and ventral side. In this study, the dorsal side of the dorsal-most raker of each middle segment of the gill arch (stubs 1D, 2D, 3B, 4B; Figure 8A) was used based on the assumption that water flow over the raker structures is greatest at the midpoint of each arch. For cell type comparison, the total number of denticles was counted on the entire raker of each gill arch section used and 27 SEM images were taken for each raker. Nine images were obtained at the most anterior denticle (furthest from the gill arch), nine comparable images were taken at the denticle halfway between the most posterior and anterior denticles on the raker, and a set of nine comparable images were collected at the most posterior denticle (closest to the gill arch). The specific magnifications and locations of these images can be found in Figure 8C. A range of magnifications was taken at each location to allow comparison of the tissue and cell types. 214x magnification of the raker at the base, middle, and tip of each observed arch section provided a complete view of the general features on the whole raker tissue section including denticles and pavement cell density. 500x magnification on sections medial and lateral to the denticle provided appropriate images for counting mucous cells. 1290x and 3460x magnifications both provided detailed views of specific cell types of interest including mucous cells and chloride cells on the gill raker. Each of these magnifications provided a detailed view of

distinct characteristics of specific cell types and microstructures, which were used to compare with SEM images from the literature.

Mucous Cell Quantification

To quantify the mucous cell density in the locations medial and lateral to the denticle on the gill raker, SEM images were collected and analyzed using ImageJ (OS version), a Java-based image processing program provided by the National Institutes of Health. This free program was downloaded from <http://rsb.info.nih.gov/ij/>. The analysis plugin “Cell Counter” was downloaded from <http://rsb.info.nih.gov/ij/plugins/index.html> once ImageJ was installed. To analyze a single location, the SEM image was opened in the ImageJ program and calibrated. A line was drawn to match the length of the 10 μm scale bar on the SEM image and Analyze > Set Scale was selected from the program main menu bar to provide a value for the number of pixels per micron. This pixels/ μm value was based on the length of the line drawn to match the scale bar. Next, the total area of the image was measured by selecting the rectangular selection tool, dragging the rectangle tool to outline the entire area of the SEM image, and then selecting Analyze > Measure. This provided the total area of the image in square microns. The area of any damaged sections of the image was then measured using the polygon and freehand selection tools, selecting Measure from the Analyze toolbar, and subtracting this damaged area from the total area to provide the total usable area of the image. Next, the Cell Counter feature was opened by selecting Plugins in the top menu > Analyze > Cell Counter. The Initialize button was selected to configure the SEM image with the plugin. Next, a counter mark was placed next to each of the mucous cells on the usable portion of the image. Cell Counter provided the total number of marks made in the “Type 1” row of

the “Counters” box in the left column of the plugin. Once all mucous cells were counted, the image was saved. Finally, a value for each image was calculated by dividing the total usable area (in square microns) by the total number of mucous cells counted in that usable area to provide the area one would have to search to find a single mucous cell in that particular location on the raker. Data were recorded in Microsoft Excel.

Statistical analysis was performed in JMP (version 10.0). The values for the areas containing mucous cells were first log transformed due to unequal variance of the raw data. Once transformed, a two-way Analysis of Variance (ANOVA) was performed with the dependent variable as the log of the area and the independent variables as the arch number and location (tip, middle, or base) on the raker. The streamwise location (i.e., medial vs. lateral to the denticle) on the raker was a crossed factor. When an ANOVA was significant ($p \leq 0.05$), Tukey-Kramer HSD testes were used to determine whether mucous cell density differed significantly in pairwise comparisons. An alternative method to assess the variance could have included an analysis of covariance (ANCOVA) to account for the two sources of error in the ratio of mucous cells per usable area.

Results

Pavement Cells

Pavement cells were characterized by a distinctive fingerprint pattern made from the arrangement of microridges, or micropilae, in concentric circles within each cell. Comparison of SEM images with existing literature confirmed the presence of this distinct cell type on the gill rakers of all specimens in this study. While there are general characteristics of this cell type as shown in Figure 9, a wide variation in the density of microridges per pavement cell, total number of pavement cells per area, and structure of

individual cells medial vs. lateral to the denticle was observed at different locations on the raker.

SEM images were obtained from the dorsal side at the tip, middle, and base location of each raker. Images were taken medial and lateral to each denticle to compare the tissue composition of each region. This revealed distinct microridge, total pavement cell density, and cell structure differences between these medial and lateral locations across all four arches of each specimen. SEM images of the epithelial tissue medial vs. lateral to the denticle at the tip of the raker on Specimen VII showed a clear distinction between the evenly spaced and sized cells medial to the denticle and the varied depth and shape of cells lateral to the denticle (Figure 10). The epithelial tissue medial to the denticle exhibited pavement cells with a high density of microridges organized homogeneously throughout the tissue. The height of each cell was equal and as a result, the entire sheet of tissue was flat and level throughout. The tissue lateral to the denticle exhibited cells with distinct depth variations including cells slightly concave and sunken inwards and other cells raised above the plane of the raker. Similar observations were made at the middle raker location.

The density of microridges in individual cells was also clearly different between the regions medial vs. lateral to the denticle at the mid-raker location. The microridges of medial cells were arranged in an even and consistent pattern whereas some pavement cells in the lateral region either had microridges concentrated towards the center of the cells or had widely-spaced microridges. Similar to the tip location, the shape and structure of the pavement cells medial to the denticle at the middle raker location were also observed to be uniformly circular and even in depth. A number of the lateral cells

were flat. However, some had a concave or depressed appearance. All of the pavement cells medial to the denticle appeared in an even circular shape. However, some lateral cells displayed a less circular shape and instead appeared to be longer and stretched out or hexagonal (Figure 11).

The base of the raker location displayed a similar trend of differences between microridge density. However, it appeared that there was less variation in cell structure between the medial and lateral locations. Some microridges of individual pavement cells lateral to the denticle were more closely clustered towards the center of the cell while microridges in other cells were more widely-distributed (Figure 12). Pavement cells at the base location were neither raised up nor sunken as was observed lateral to the denticle at the middle and tip locations. Figures 10-12 were from the first and second arch and a similar pattern was also observed on the third and fourth arch.

Mucous Cells

Upon initial SEM investigation, an unknown cell type was detected at a relatively high frequency across SEM stubs. Small structures emerged from the subepithelial layer of this cell type, which resembled microvilli of taste buds. However, the oral morphology literature also identified mucous cells that secreted mucous granules from the subepithelial layer. An extensive comparison was conducted using images from the scientific literature on fish oral cavities. Image libraries for both mucous cells and taste buds were compiled from a variety of fish species and used for comparison with SEM images acquired in this study. Species documented in the literature ranged from members of the family Atherinopsidae to the family Bagridae. Although both of these cell types are known to vary between species, images from a diversity of fish species showed general

morphological similarities and the libraries were thus deemed a reliable source with which to compare images collected in this study. Comparisons revealed that the microvilli of taste bud cells were less than 0.5 μm (Kang et al., 2013), which was substantially smaller than the 10 μm mucous secretion clusters observed in the American shad. In addition, taste buds have not been reported on the gill rakers of fish species in the literature, while mucous cells were consistently documented throughout the gill structures of multiple species. This information has established that the cell types observed in collected American shad specimens were most likely ruptured mucous cells with the subepithelial mucous secretions present as clustered globules (Figure 13).

During observations of pavement cell densities across the gill raker, a distinct mucous cell patterning was also distinguished. A consistent pattern of fewer mucous cells medial to the denticle and more mucous cells clustered lateral to the denticle was observed in Spring 2012 (Figure 14A). In Fall 2012, additional SEM images were collected at 500x magnification medial and lateral to the denticle at the tip, middle, and base positions on the raker on all four arches of all five specimens to confirm this trend (Figure 14B). Graphical and statistical analysis confirmed that there is a difference in mucous cell density between these two locations. The mucous cell density is greater lateral to the denticle for all four arches and across all three locations. Graphical representations of these data are shown in Figure 15 where the mean mucous cell density on each arch is depicted at the tip, middle, and base locations. A series of statistical analyses were performed to interpret the data. A two-way ANOVA in combination with Tukey-Kramer pairwise comparison revealed that the mucous cell distribution at the tip of the raker was significantly different from the middle and base locations ($p < 0.0001$).

The mucous cell distribution was not significantly different between the middle and base positions of the raker. Mucous cell densities were significantly different medial to the denticle vs. lateral to the denticle ($p < 0.0001$). There was no difference in mucous cell density between the four arches ($p = 0.09$).

Denticle Structure

On all observed specimens, denticles were located closer to the medial side of the raker and thus further from the lateral side of the raker (Figure 16). The total number of denticles was counted and recorded on each of the 20 rakers examined in this study. For each specimen, each raker decreased in total length from the first to the fourth gill arch. The gill rakers farther anterior had a greater total denticle count compared to rakers more posterior in the oral cavity. Rakers with shorter total length have less tissue and therefore exhibit fewer denticles. The mean value of denticle total was calculated for each arch (Figure 17). Arch 1 had the most denticles and the mean denticle total decreased from Arch 2 to Arch 4. However, the greatest difference between adjacent rakers was from Arch 1 to Arch 2. Although not directly measured, it appears that all denticles are an equal distance from the medial edge of the raker and this is consistent for the entire raker and across all four gill arches.

Chloride Cells

Chloride cells have been reported previously in scientific literature to be abundant on the gill filaments but generally absent on the gill rakers. Based on the morphological similarities between SEM images collected in this study, chloride cells described in the literature, and a compiled chloride cell library, there is strong evidence to suggest that chloride cells appear on the gill rakers of the American shad. These cells are distinctly

different from mucous cells based on their size, shape, and frequency of appearance on the American shad raker. Unlike the unruptured and ruptured mucous cells (Figure 14) that are approximately 10 μm , the cells that are tentatively identified as chloride cells in American shad are approximately 2 μm in width (Figure 18). Suspected chloride cells appeared to be sparsely and nonspecifically distributed on the raker tissue. There was no specific location on the raker where these cells were observed more frequently. These cells were significantly less abundant than mucous cells. However, it is also possible that they are more frequently unidentified given their small size and their less easily recognized structure.

Discussion

Pavement Cells

Pavement cells form the epithelial tissue that spreads across 90% of the gill raker while the remainder of the raker is covered in mucous cells, chloride cells, and denticle structures (Wilson and Laurent, 2002). These cells are found on the surface of gill tissue and skin of all fish species while scarcely found in other members of the animal kingdom (Bradley, 2009). Characteristically hexagonal in shape, pavement cells range from 5-15 μm in width (Olson, 1996). Each of these characteristics were essential in identifying the pavement cells in the American shad specimens.

The difference in microridge density and cell structure medial vs lateral to the denticle at tip, middle, and base locations on the raker could indicate a particular function of distinct regions of the raker. Inside the American shad oral cavity, water flows in towards the rakers and meets the row of denticles on the medial side of the raker followed by the epithelial tissue lateral to the denticle. The results presented in this study raise the

question of whether there is a correlation between the role of the denticle and the density of pavement cells involving specific interactions with the water flowing through the oral cavity. Pavement cells have been suspected to play a role in gas transfer across the epithelial layer and possibly contribute to acid-base ion regulation. However, these functions have been documented only on the gill lamellae in fish oral morphology literature (Evans et al., 1999). This hypothesized function of pavement cells as pH regulation mechanisms on the gill lamellae suggests that pavement cells throughout the oral cavity could play a similar role in gas transfer and pH regulation across the epithelial layer. Pavement cells medial to the denticle would be the first pavement cells to meet this incoming water and could therefore play a more significant role in acid-base regulation compared to pavement cells further downstream.

Olson (1996) suggested additional possibilities for microridge function including an ability to increase the flexibility and surface area of the tissue given the characteristic folded surface of the microridges in pavement cells. Although it is highly speculative and there is insufficient data to address the question, the region medial to the denticle may experience greater movement including bending and curving given its interaction with the incoming water flow. Increasing the flexibility of these cells with a high microridge density might reduce tissue damage given that more flexible tissue could withstand changes in structure resulting from disruption by water flow.

Microridges of pavement cells are also suspected to sequester and hold mucous granules that are being secreted from mucous cells (Olson, 1996). More densely clustered microridges medial to the denticle could serve to more effectively trap mucous from the fewer mucous cells that are present in that location, relative to the area lateral to the

denticle. The medial region may be subject to a higher velocity of water flowing over the cells, and these microridges may aid in preventing this mucous from being dislodged.

The growth pattern of gill rakers is currently uncertain. However, it is possible that the microridge density patterns could be a result of the growth of the gill raker in a specific manner. For example, the medial tissue could be the oldest tissue, which might explain the higher microridge density of medial pavement cells compared to the newer tissue downstream on the raker towards the lateral side. Future research on gill raker development is necessary to answer this question.

Although there was an observed difference in pavement cell and microridge structure medial vs. lateral to the denticle, it is also important to consider the possibility that these differences may be an artifact of the preservation process. Tissue locations with a higher mucous cell density would be more susceptible to tissue distortion during the dehydration and preservation process. Further investigation is required to test this hypothesis.

Mucous cells

Mucous cells have proven to be extremely important for aquatic species. Mucous is a buffer between epithelial tissue and the environment, acts as a protective coat to prevent abrasions, and serves an immunological function by secreting immunoglobulin (Olson, 1996). It is also a “substrate in which antibacterial mechanisms can act” (Tort et al., 2003). The presence of these mucous cells on the gill raker is not unexpected given the numerous functions this cell type is known to perform in the oral cavity. However, the density of these cells medial and lateral to the denticle has not been examined in any

previous study. The significant difference in mucous cell density on the medial vs. lateral surfaces of the American shad gill rakers is unexpected and deserves further study.

Given that function for a higher density of mucous cells on the downstream surfaces of the gill rakers has not been evaluated, an overview of potential functions is presented here. Mucous cells concentrated on the lateral portion of the raker could lubricate the downstream surface and increase water flow. The high density of mucous cells could produce a high volume of mucosal secretions that covers the raker surface and decreases the drag as water moves across the raker.

With water and particles entering the oral cavity, the mucous from these cells could act to coat particles as they pass over the raker and allow these particles to continue to flow more easily flow towards the esophagus. Coating these particles in mucous may also act as a protective mechanism to reduce the damage that these particles might have on other tissues as water flows towards the back of the mouth. However given the low level of interaction these particles are suspected to have with oral tissues this is less likely (Brainerd, 2001).

One distinct disparity revealed through statistical analysis is the significant difference between the mucous cell densities at the tip vs. the middle and base regions of the raker. Although raker development has not been extensively documented in the current literature, a hypothesis for this pattern in mucous cell density could involve a specific mechanism of raker development. For example, if the rakers grow from the tip, and if newer tissue has fewer mucous cells, then the observed pattern in mucous cell density could result. Further research on the development of rakers must be conducted to test this hypothesis.

Chloride Cells

Chloride cells are commonly documented on the gill filaments in fish oral morphology literature including studies on development of chloride cells in larval and juvenile American shad (Zydlewski and McCormick, 1997, 2001). These limited sources only refer to this cell type on the gill filament and do not refer to chloride cells specifically appearing on the gill raker. The main function of these cells is to regulate pH and ion balance. Chloride cells have been classified into two categories in fish oral morphology literature, and both types can be found in a single fish specimen. One category is identified as surface cells, which appear on the outer epithelial layer and are more abundant in freshwater species. In contrast, recessed cells are invaginated into subepithelial apical crypts and are found more often in saltwater species (Olson, 1996). These apical crypts are known to respond by expanding in lower pH environments and contracting in more neutral conditions in teleost species (Daborn et al., 2001). However, the relationship between surface and recessed cell types still remains unclear. Although chloride cells are more abundant on the gill lamellae, it is possible that they can be found at other locations (Perry, 1997). This statement suggests that the gill raker could be a possible location on which chloride cells could be found.

Based on previous studies of other species, surface chloride cells were observed in freshwater habitats while recessed chloride cells were documented in fish specimens in saltwater environments (Olson, 1996). A very low frequency of surface chloride cells was observed in American shad and no recessed chloride cells were detected in this study. These findings are reasonable given the low salinity levels in the freshwater river where the specimens were collected and the lowered ion regulation required in a relatively

neutral aquatic environment. Previous studies were conducted in species including tilapia (*Oreochromis mossambicus*) to investigate the change in chloride cell density in freshwater and saltwater environments. Results revealed an increase in size and number of recessed chloride cells in environments of higher salinity. When placed in a freshwater environment, these recessed cells became less visible and the chloride cells became covered by the pavement cell layer. Specimens that were transferred from a high to low saline environment exhibited changes in chloride cell composition in less than an hour. (Daborn, et al., 2001). However, conflicting results were observed in the developing American shad where chloride cells were observed in freshwater, but disappeared when specimens were acclimated to seawater (Zydlewski and McCormick, 2001). The literature supports the possible presence of chloride cells in the freshwater-adapted American shad. American shad specimens would need to be collected from saltwater environments and examined under a scanning electron microscope to investigate the chloride composition in that environment. Identifying the chloride cell composition in fresh and saltwater environments would provide insight into the function of this cell type in American shad.

Denticles

Denticle structures are found on the dorsal and ventral surfaces of the gill raker in American shad. These structures have not been described frequently in fish oral morphology literature but can be identified by their tooth-like appearance projecting from the raker. Although the function of denticles is unclear, these structures are thought to influence the hydrodynamic drag as water flows across the raker surface but could also serve to protect surrounding tissues from abrasions (Atkinson and Collins, 2002). The

location of the denticle row towards the medial side of the raker and closer towards the first point of contact that incoming water has with the gill raker may indicate a specific role of these structures in the filtration of particles that enter and flow through the oral cavity. For each specimen, denticles were observed along the entire length of the raker at a relatively uniform distance from the medial edge of the raker. In addition, the denticles are oriented on the raker so that they are pointed towards the mouth of the fish and thus into the flow of water. This also might indicate a role in directing water in specific patterns through the oral cavity.

Although the majority of these denticles appeared individually along the raker, there was a less frequent occurrence of two or three denticles present at a single location in the denticle row. Understanding the developmental process of these structures may provide additional insight. The double and triple denticles appeared along random locations across the raker frequently enough to warrant further investigation into their potential role in filtering particles or altering the flow of water through the oral cavity.

Future Directions

Given the limited body of knowledge regarding the specific cell types of the gill rakers in the American shad, there are many areas left uncertain and open to future study. Specimens for this study were collected from a freshwater habitat during spawning season and thus provided data on the cell type composition of this species in freshwater. It would be useful to obtain and prepare specimens from a saltwater environment and compare the density and patterning of pavement and chloride cells from the two environments. If the findings from previous studies are correct, it is expected that recessed chloride cells would be more abundant in saltwater specimens. It would also be

expected that there would be a greater density of microridges in pavement cells across the raker given the increased demand to regulate ion concentration in saltwater.

A significant mucous cell density difference was identified in this study at locations medial vs. lateral to the denticle on the gill raker. Tissue medial to the denticle possessed a lower density of mucous cells per unit area than the tissue lateral to the denticle. This study looked at gill rakers in the middle of each arch where the water flow was presumably the greatest. Further investigation into the mucous cell density at different locations on the gill arch would give a more complete picture of the role of mucous cells in the oral cavity. Higher densities of mucous cells at locations where water flow is greater would indicate an important role of mucous cells with respect to the movement of water in the oral cavity. SEM imaging methods could be used to obtain this information.

Future studies quantifying the distance between denticles may provide information into the particle size this species could consume by using the gill rakers as a dead-end sieve. Using SEM to examine the gill rakers of varying aged specimens may also provide insight into the development of the denticle structure. This study would also provide valuable information regarding the development of the raker structure, which would provide additional information regarding the mucous cell density patterning. There are many areas that remain uncertain regarding the cell types and microstructures of American shad. Histological methods including tissue section preparation could serve as an additional technique to study cell type structure at the microscopic level. Exploration of these areas will provide deeper insight into the mechanism of feeding and the dynamics of water flow in the oral cavity as well as the role of these specific cell types

and morphological structures in these processes. Given the limited body of knowledge in the field of American shad oral morphology, these observations may ultimately contribute to future studies relating observed ultrastructure to function in this species.

Literature Cited

- ASMFC (Atlantic States Marine Fisheries Commission). 1999. Amendment 1 to the interstate fishery management plan for shad and river herring. ASMFC, Report 35, Washington, D.C.
- ASMFC (Atlantic States Marine Fisheries Commission). 2007. American shad stock assessment report for peer review, volume 1. ASMFC, Stock Assessment Report 07-01 (Supplement), Washington, D.C.
- Atkinson, C., & Collins, S. 2002. Structure and topographic distribution of oral denticles in elasmobranch fishes. *Biol Bull*, 222(1): 26-34.
- Bigelow, A. F., Schroeder, W. C., Collette, B. B., Klein-MacPhee, G., & Bigelow, H. B., 2002. Shad: The Herring and Tarpon Tribes. In *Bigelow and Schroeder's fishes of the Gulf of Maine*. (3rd ed., p. 108). Washington, DC: Smithsonian Institution Press.
- Blaber, S. J. 1997. Feeding Ecology and Trophic Structure. In *Fish and fisheries in tropical estuaries*. London: Chapman & Hall.
- Bradley, T. J., 2009. *Animal osmoregulation*. Oxford: Oxford University Press.
- Brainerd, E. L., 2012. Caught in the crossflow. *Nature*, 412: 387-388.
- Bührnheim, C. M., & Malabarba, L. R. 2006. Redescription of the type species of *Odontostilbe* Cope, 1870 (Teleostei: Characidae: Cheirodontinae), and description of three new species from the Amazon basin. *Neotropical Ichthyology*, 4(2): 167-196.
- Daborn, K., et. al, 2001. Dynamics of pavement cell-chloride cell interactions during abrupt salinity change in *Fundulus heteroclitus*. *Journal of Experimental Biology*, 204, 1889-1899.
- Evans, D. H et al. 1999. Ionic transport in the fish gill epithelium. *Journal of Experimental Zoology*, 283(7): 641-652.
- Hammann, M. Gregory. 1985. The developmental morphology of the filtering apparatus in American shad, a planktivorous fish: A Preliminary Study. *Ciencias Marinas* 11: 5-20.
- Kang, C., et al. 2013. The acute and regulatory phases of time-course changes in gill mitochondrion-rich cells of seawater-acclimated medaka (*Oryzias dancena*) when exposed to hypoosmotic environments. *Comparative Biochemistry and Physiology Part A: Molecular & Integrative Physiology*, 164(1):181-191.
- Latour, R. J., Hilton, E. J., Lynch, P. D., Tuckey, T. D., Watkins, B. E., & Olney, J. E. (2012). Evaluating the Current Status of American Shad Stocks in Three Virginia Rivers.

Marine and Coastal Fisheries: Dynamics, Management, and Ecosystem Science, 4(1): 302-311.

Olson, K. R. 1996. Scanning Electron Microscopy of the Fish Gill. In *Fish Morphology: Horizon of New Literature* (pp. 31-45). Enfield, NH: Science.

Perry, S. 1997. The Chloride Cell: Structure and Function in the Gills of Freshwater Fishes. *Annual Review of Physiology*, 59: 325–347.

Sanderson, S., Cheer, A., Goodrich, J., Graziano, J., Callan, T. 2001. Crossflow filtration in suspension-feeding fishes. *Nature* 412: 439-441.

Stangl, M. 2012. American Shad Restoration on the Nanticoke River. *Delaware Department of Natural Resources and Environmental Control (DNREC)*. Retrieved from http://www.dnrec.delaware.gov/fw/Fisheries/Documents/Shad_Flyer.pdf

Storm, T. 2009. Oral Morphology of the Suspension-feeding American shad, *Alosa sapidissima*.

Tort, L., Balasch, J., Mackenzie, S. 2003. Fish immune system. A crossroads between innate and adaptive responses. *Immunología*, 22: 277-287.

Wilson, J., Laurent, P. 2002. Fish Gill Morphology: Inside Out. *Journal of Experimental Zoology*, 293: 192-213.

Zydlewski, J., & McCormick, S. D. (2001). Developmental and environmental regulation of chloride cells in young American shad, *Alosa sapidissima*. *Journal of Experimental Zoology*, 290(2): 73-87.

Zydlewski, J., & McCormick, S. D. (1997). The ontogeny of salinity tolerance in the American shad, *Alosa sapidissima*. *Can. J. Fish. Aquat. Sci.*, 54: 182-189.



Figure 1: Fresh specimen with operculum removed to show the natural orientation of the gill arch in the oral cavity. Gill rakers are the white structures attached to the gill arch and pointing towards the anterior (the opening of the mouth). Gill filaments are the red feather-like structures pointing towards the posterior of the specimen.

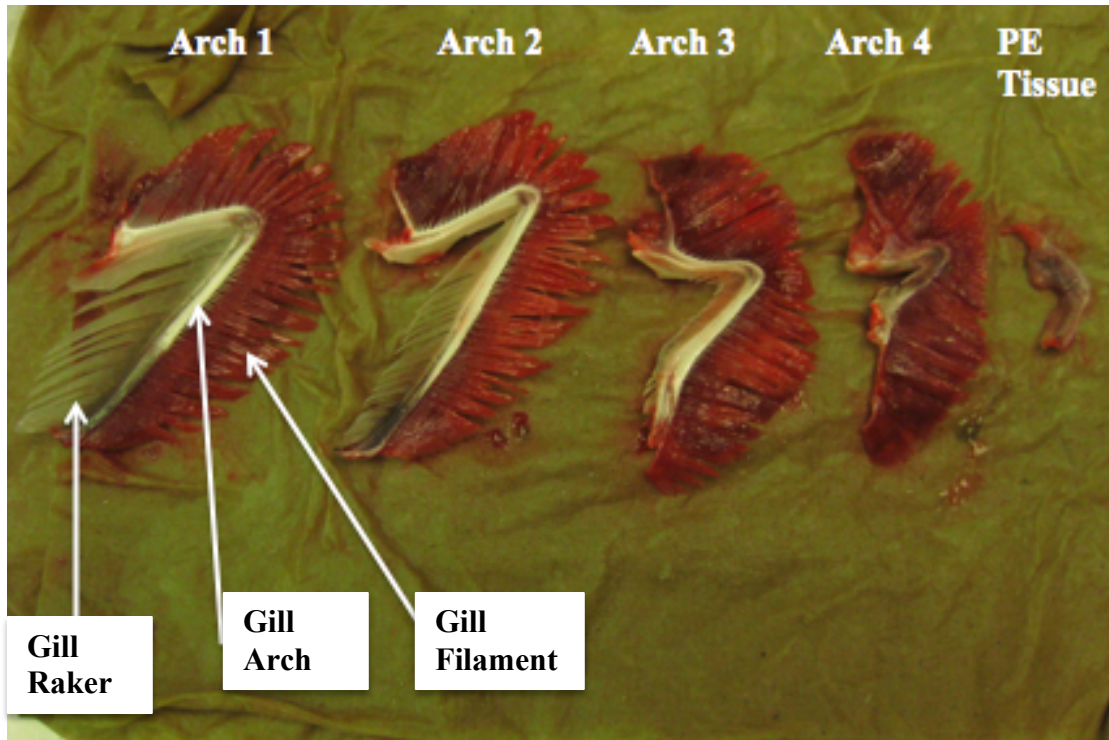


Figure 2: Four gill arches and the pre-esophageal tissue removed from the specimen. Gill arches were cut into small sections to allow for mounting onto SEM stubs. Gill raker, arch, and filament are labeled.

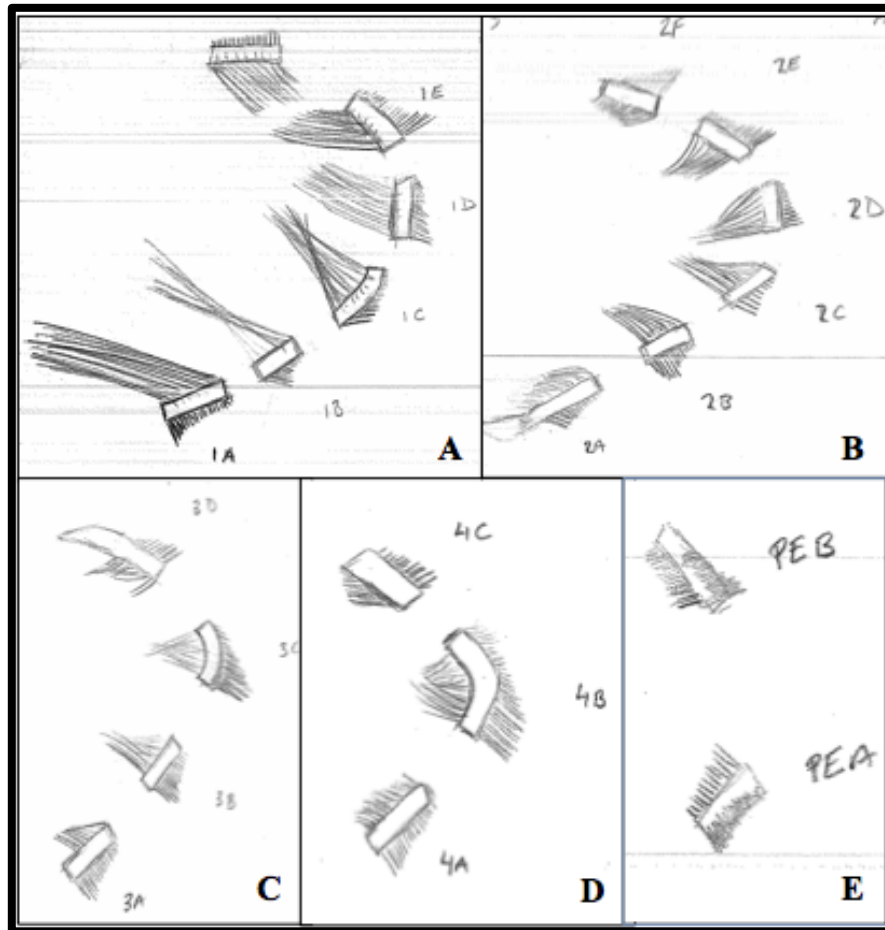


Figure 3: Diagram of the stub sketches for specimen I. The first four gill arches (boxes A, B, C, and D) were mounted to provide a lateral view of the rakers. The dorsal end of the gill filaments on each stub was cut shorter to provide a reference under the SEM. The pre-esophageal tissue was mounted to show the anterior view.

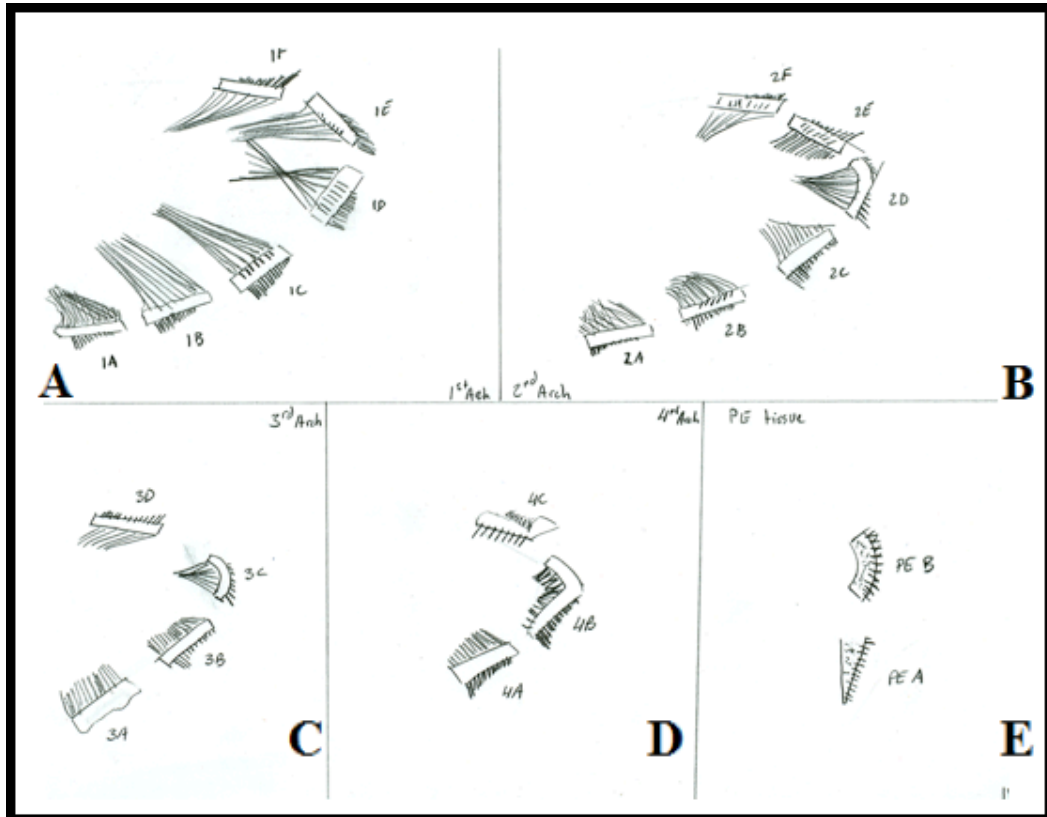


Figure 4: Diagram of the stub sketches for specimen IV drawn by Storm (2009). The first four gill arches (boxes A, B, C, and D) were mounted to provide a lateral view of the rakers. The dorsal end of the gill filaments on each stub was cut shorter to provide a reference under the SEM. The pre-esophageal tissue was mounted to show the anterior view.

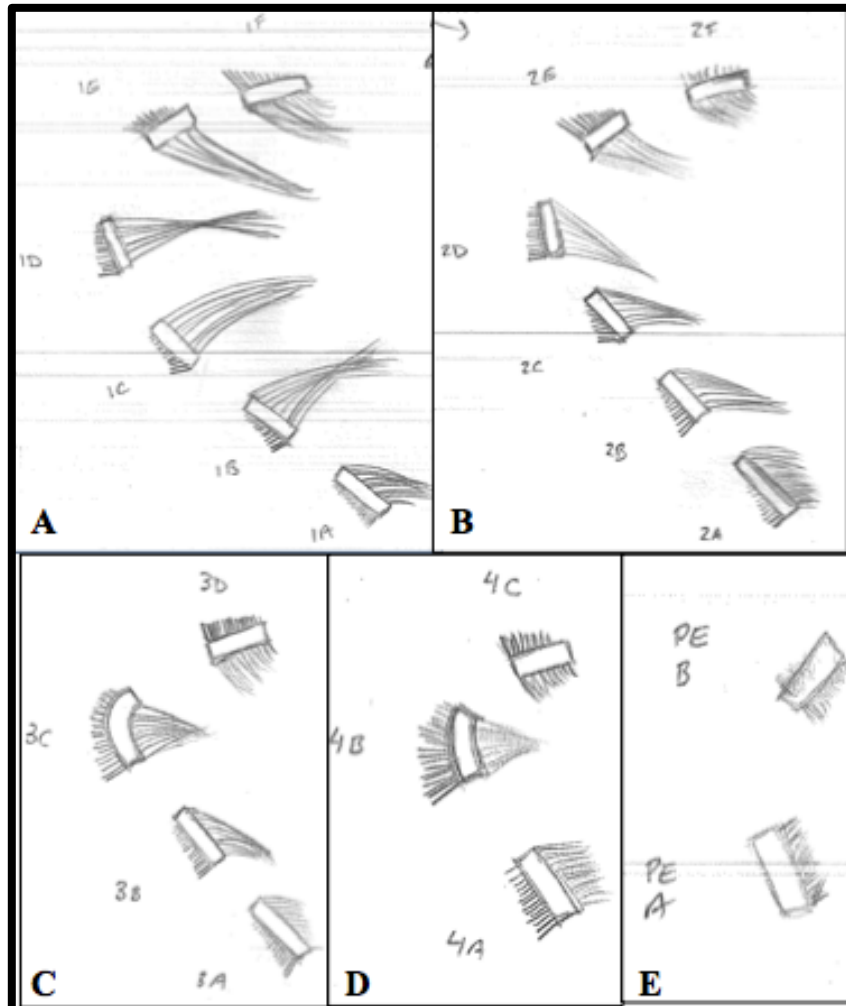


Figure 5: Diagram of the stub sketches for specimen II. The first four gill arches (boxes A, B, C, and D) were mounted to provide a medial view of the rakers. The dorsal end of the gill on each stub was cut shorter to provide a reference under the SEM. The pre-esophageal tissue was mounted to show the anterior view.

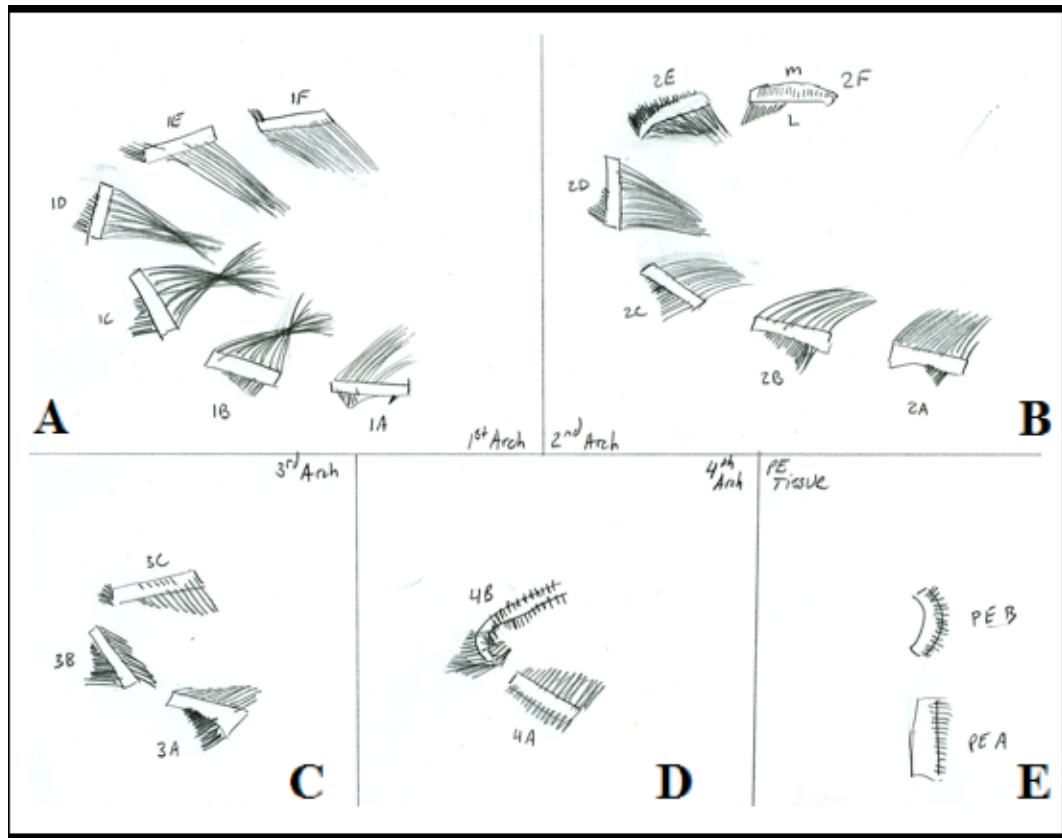


Figure 6: Diagram of the stub sketches for specimen VI drawn by Storm (2009). The first four gill arches (boxes A, B, C, and D) were mounted to provide a medial view of the rakers. The dorsal end of the gill filaments on each stub was cut shorter to provide a reference under the SEM. The pre-esophageal tissue was mounted to show the anterior view.

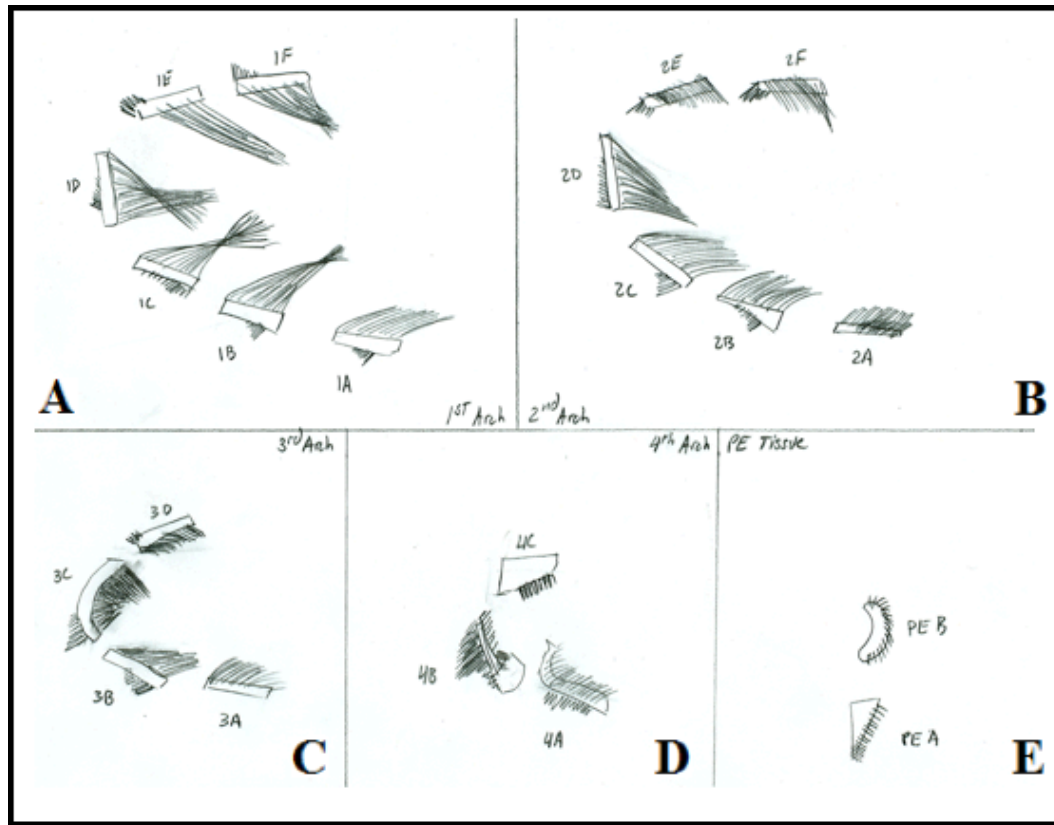


Figure 7: Diagram of the stub sketches for specimen VII drawn by Storm (2009). The first four gill arches (boxes A, B, C, and D) were mounted to provide a medial view of the rakers. The dorsal end of the gill filaments on each stub was cut shorter to provide a reference under the SEM. The pre-esophageal tissue was mounted to show the anterior view.

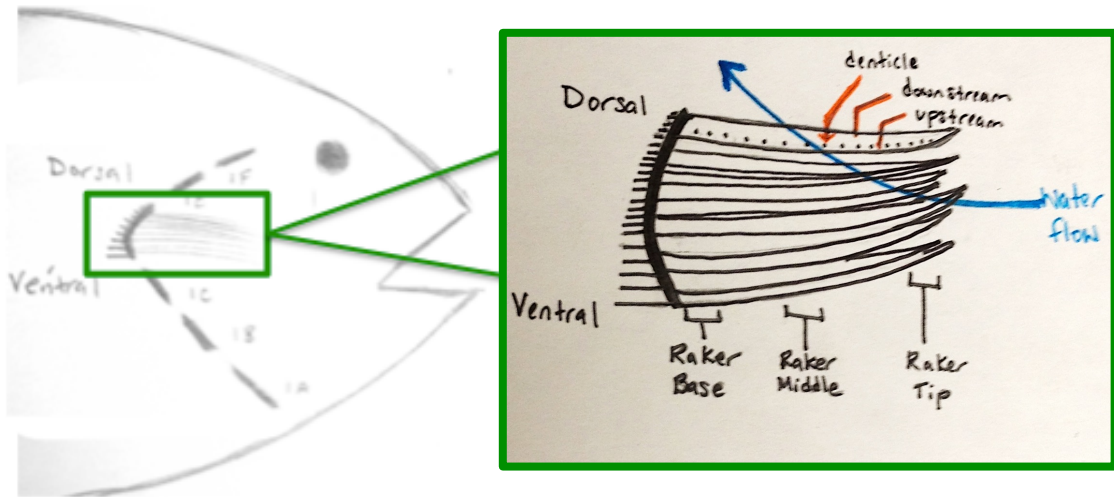


Figure 8A: (Left)
 Diagram shows the location of the left gill arch sections used from each specimen. An enlarged view of the stub shows a medial view of the gill arch including the upstream (medial of the denticle) and downstream (lateral of the denticle) locations.

Figure 8B: (Right)
 Image of one specimen stub as observed in the SEM. Stub mounted to provide a medial view with the denticles closer to the medial side of the raker. Image magnified in Figure 8C to indicate exact imaging locations.

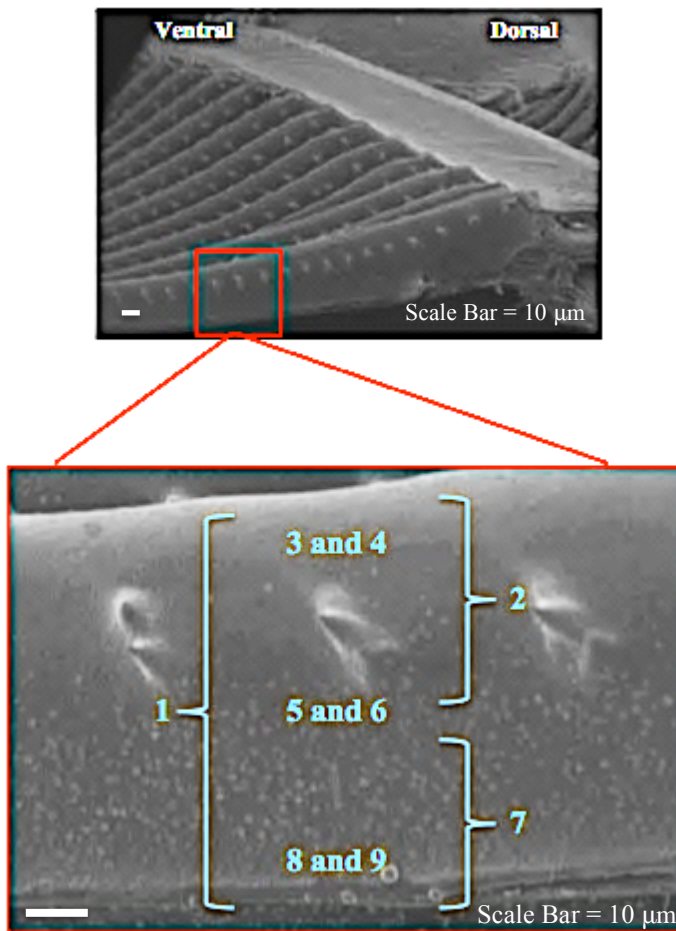


Figure 8C: SEM Imaging Locations

1. 214x- Entire raker
2. 500x- Denticle and most upstream region
3. 1290x- Directly above denticle
4. 3460x- Directly above denticle
5. 1290x- Directly below denticle
6. 3460x- Directly below denticle
7. 500x- Most downstream region
8. 1290x- Most downstream region
9. 3460x- Most downstream region

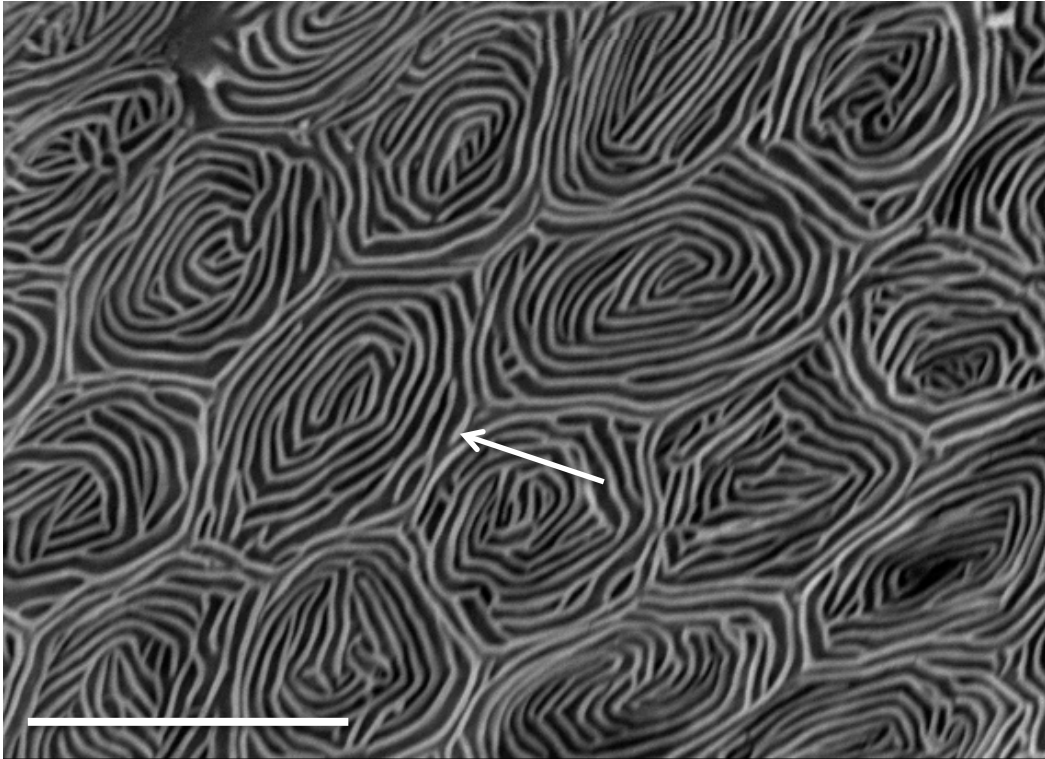
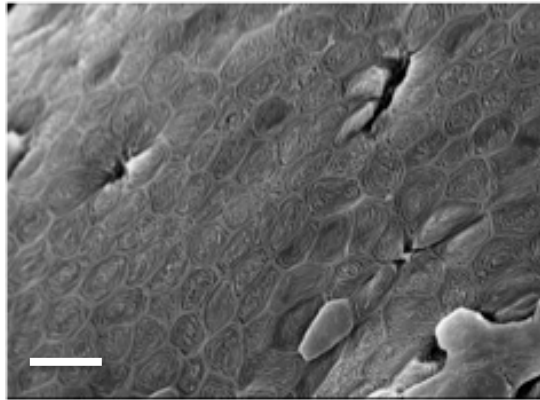
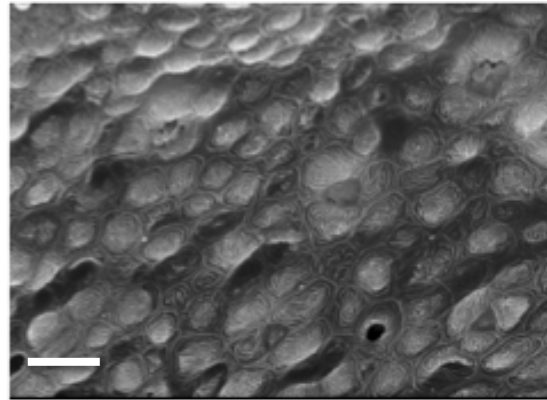


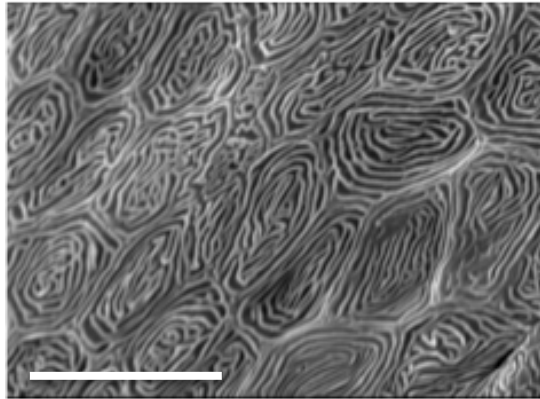
Figure 9: Pavement cells as observed under the SEM with characteristic concentric circles of the microridges (arrow). Scale bar 10 μm .



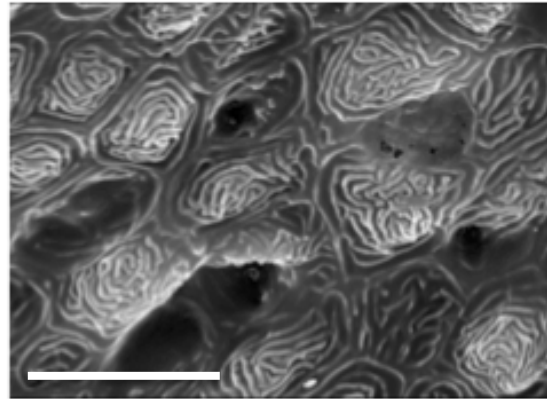
A- Tissue directly above denticle, 1290x



B- Tissue directly below denticle, 1290x



C- Tissue directly above denticle, 3460x



D- Tissue directly below denticle, 3460x

Figure 10: Pavement cell density medial of the denticle (A and C) and lateral of the raker (B and D) at the tip location. Scale bar 10 μm .

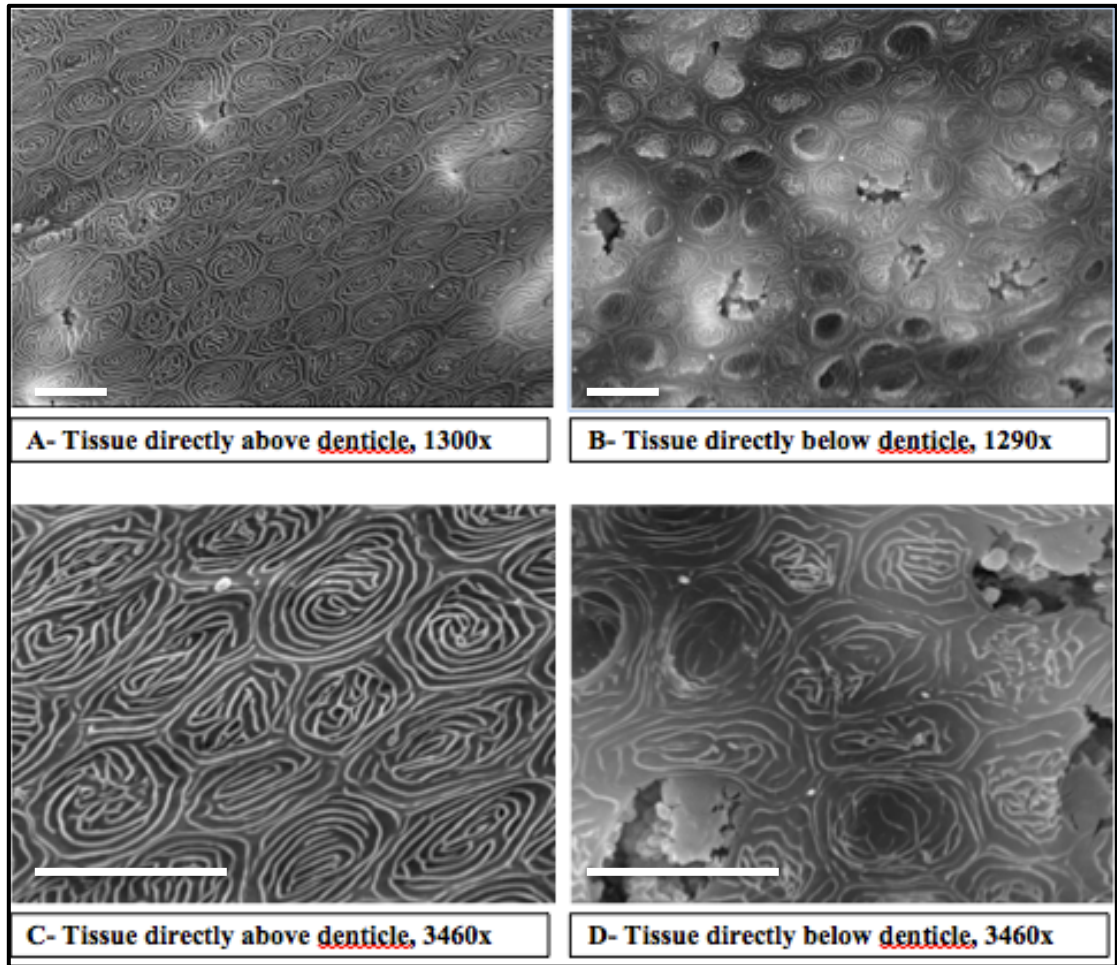


Figure 11: Pavement cell density medial of the denticle (A and C) and lateral of the raker (B and D) at the middle location. Scale bar 10 μm .

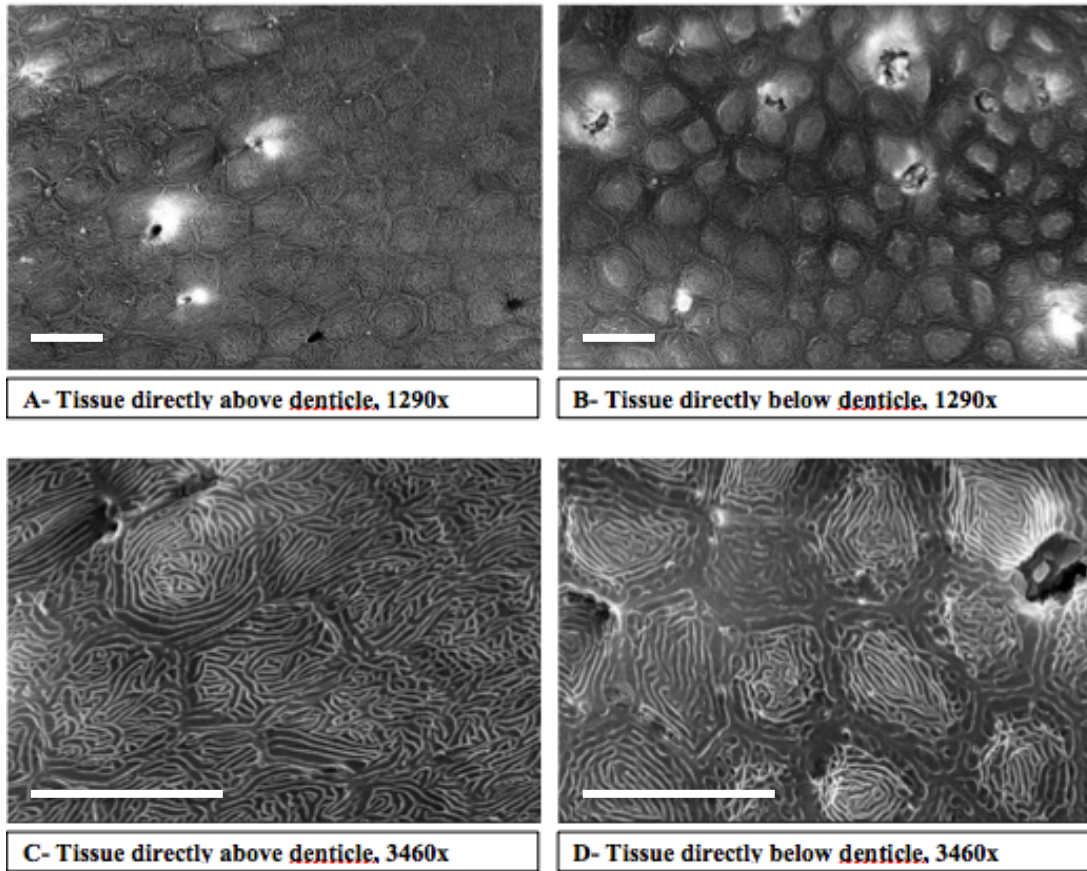


Figure 12: Pavement cell density medial of the denticle (A and C) and lateral of the raker (B and D) at the base location. Scale bar 10 μ m

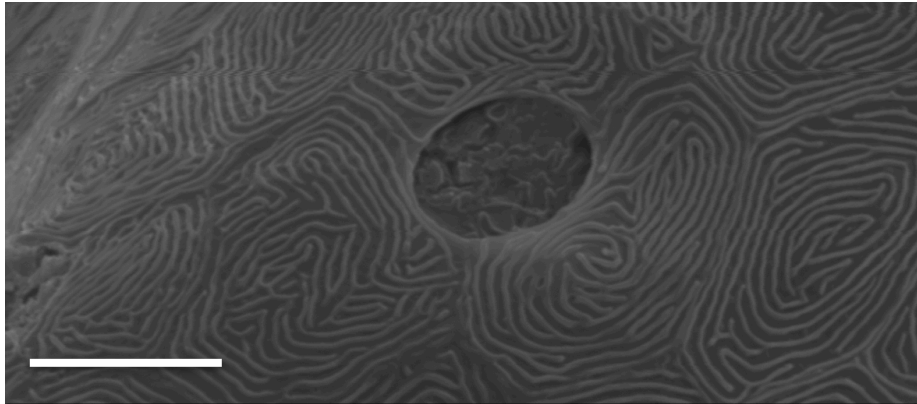


Figure 13A: Non-ruptured mucous cell with mucous granules visible on the subepithelial layer. Scale bar 10 μm .

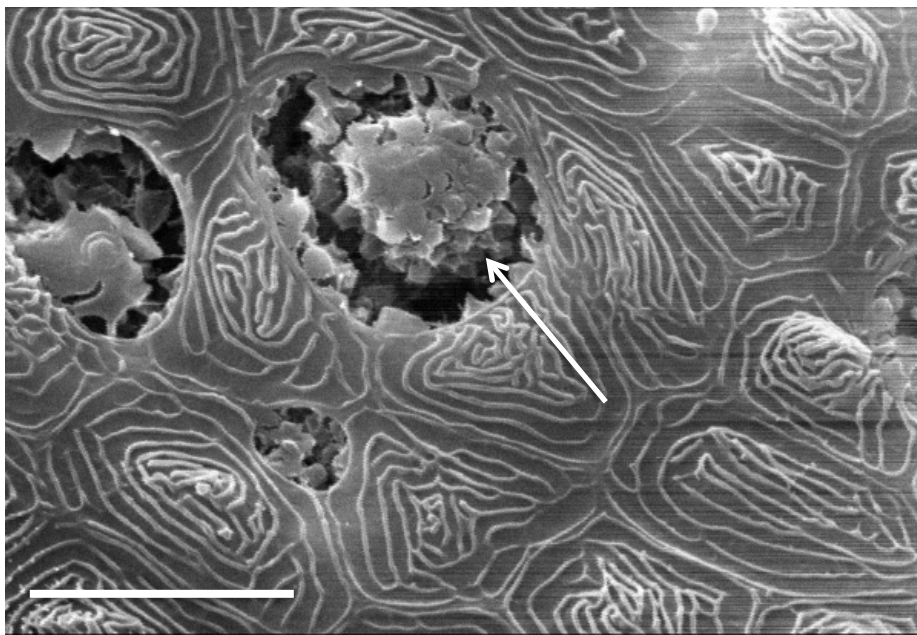


Figure 13B: Ruptured mucous cells with globular secretions (arrow). Scale bar 10 μm .

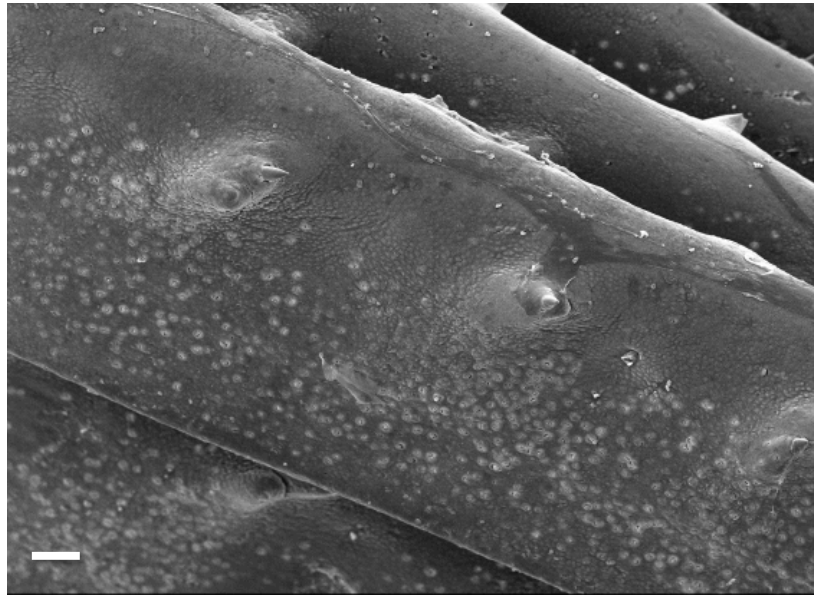


Figure 14A: Mucous cell gradient at the middle location of the raker. Denticles are shown positioned towards the medial side of the raker. Scale bar 10 μm .

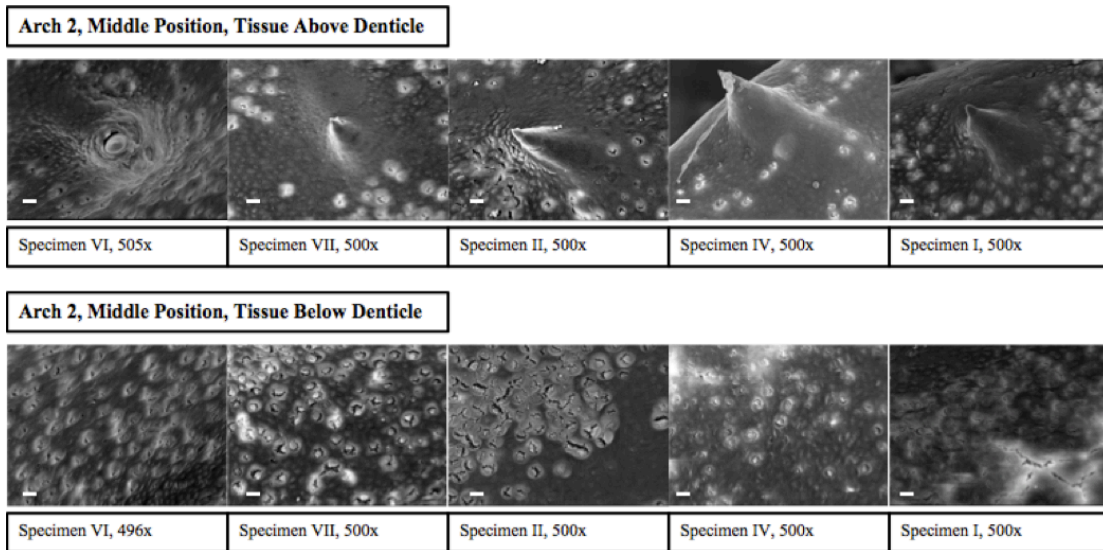


Figure 14B- Mucous cell gradient for specimens I, II, IV, VI, and VII in the middle location. Top row shows SEM images from location medial of the denticle and the bottom row shows images from locations lateral of the denticle. Scale bar 10 μm .

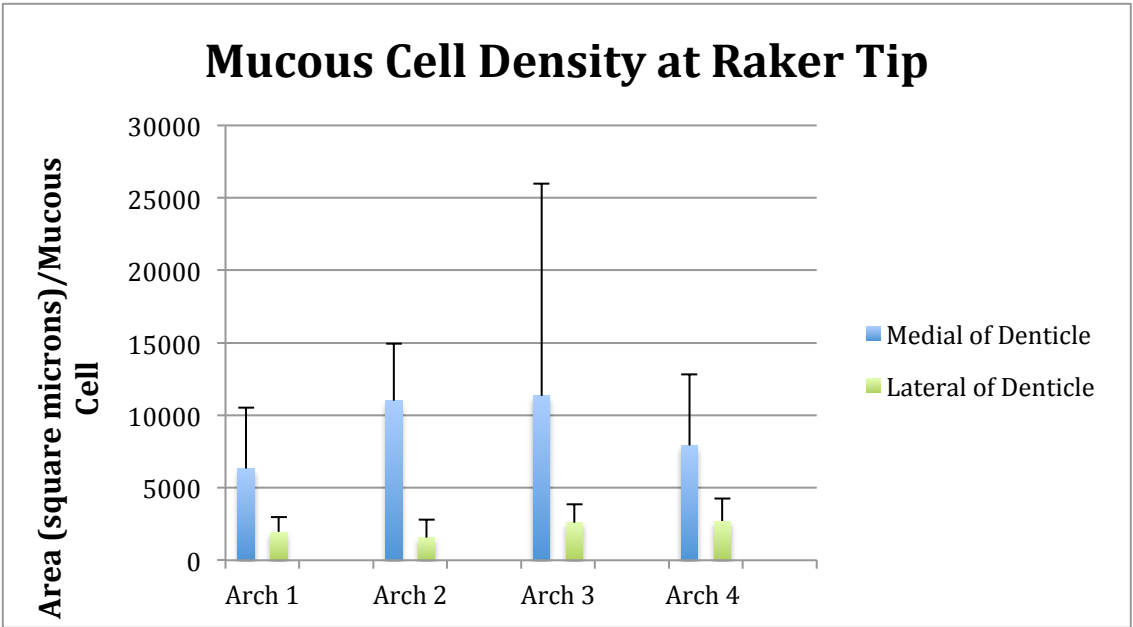


Figure 15A: Graph represents the total area in which a single mucous cell would be found at the tip of the raker. Blue bars represent the mean value of all five specimens at the tip location on each arch medial of the denticle. Green bars represent the mean value of all five specimens at the tip location on each arch lateral of the denticle. Bars represent standard deviation.

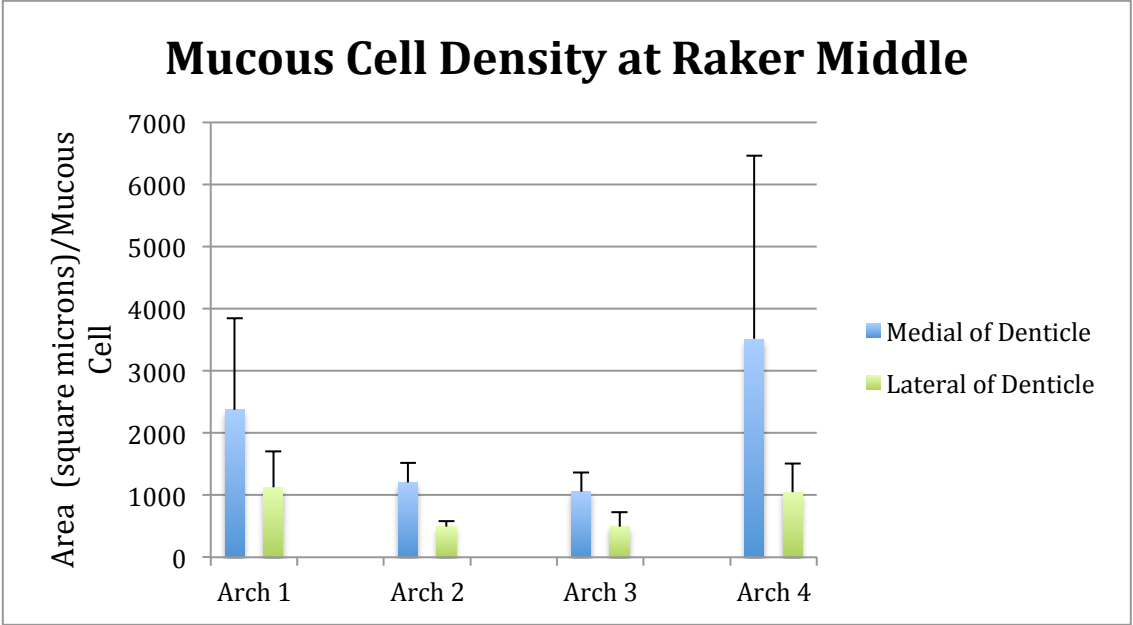


Figure 15B: Graph represents the total area in which a single mucous cell would be found at the middle of the raker. Blue bars represent the mean value of all five specimens at the middle location on each arch medial of the denticle. Green bars represent the mean value of all five specimens at the middle location on each arch lateral of the denticle. Bars represent standard deviation.

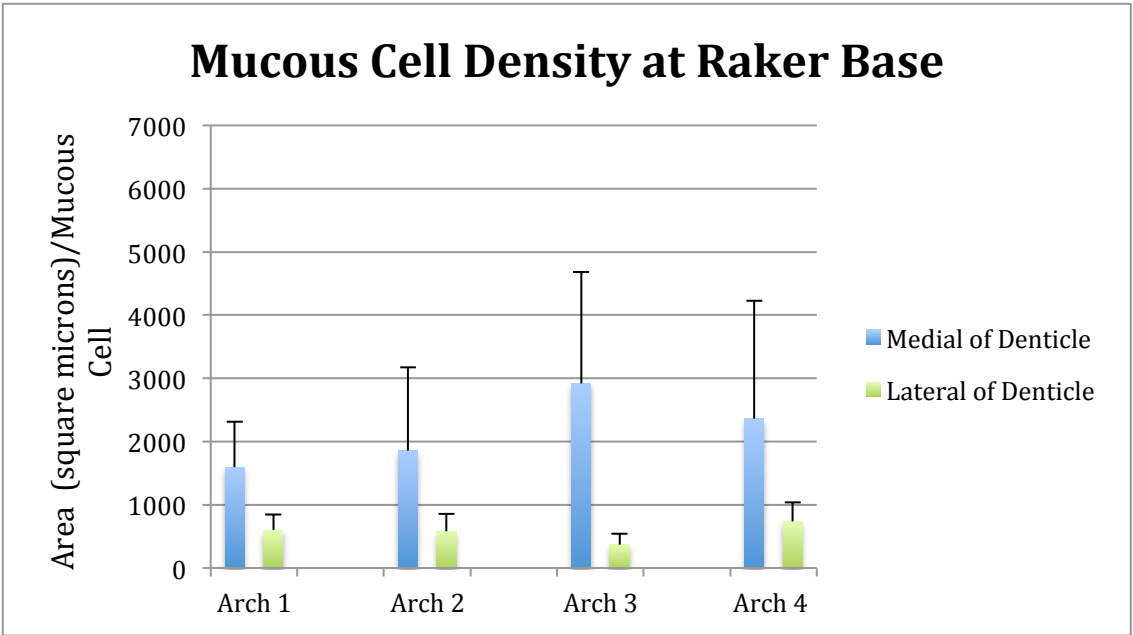


Figure 15C: Graph represents the total area in which a single mucous cell would be found at the base of the raker. Blue bars represent the mean value of all five specimens at the base location on each arch medial of the denticle. Green bars represent the mean value of all five specimens at the base location on each arch lateral of the denticle. Bars represent standard deviation.

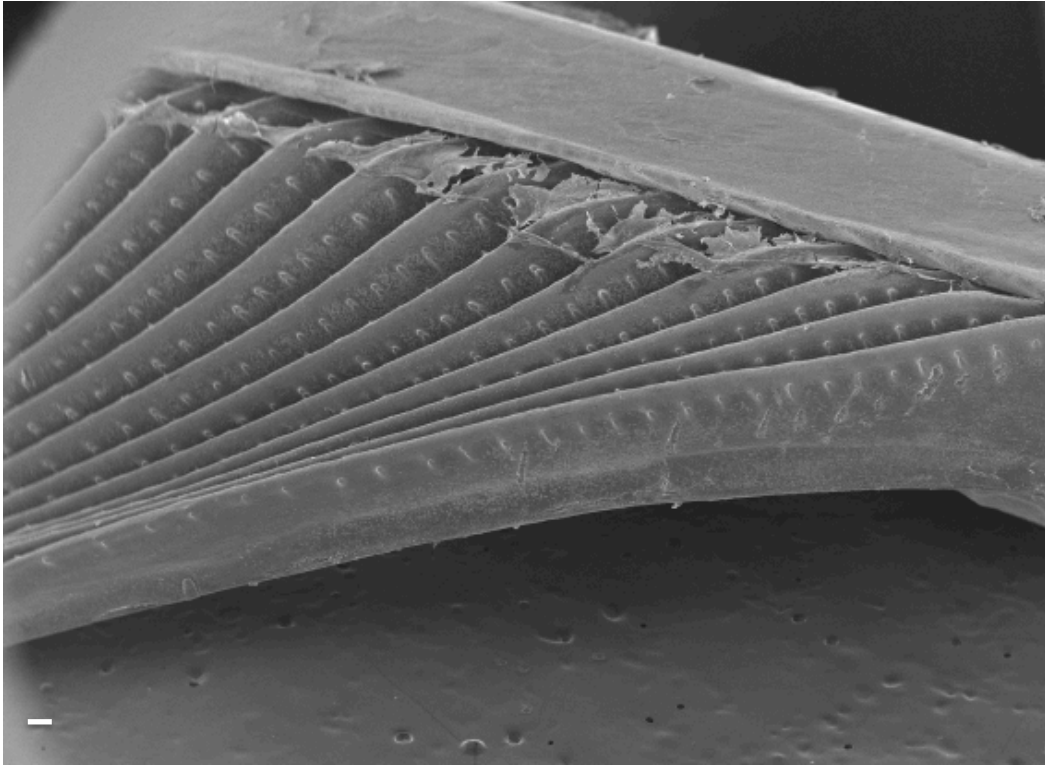


Figure 16: SEM of an entire stub with the denticle location shown closer to the medial side of the raker. Scale bar 10 μm .

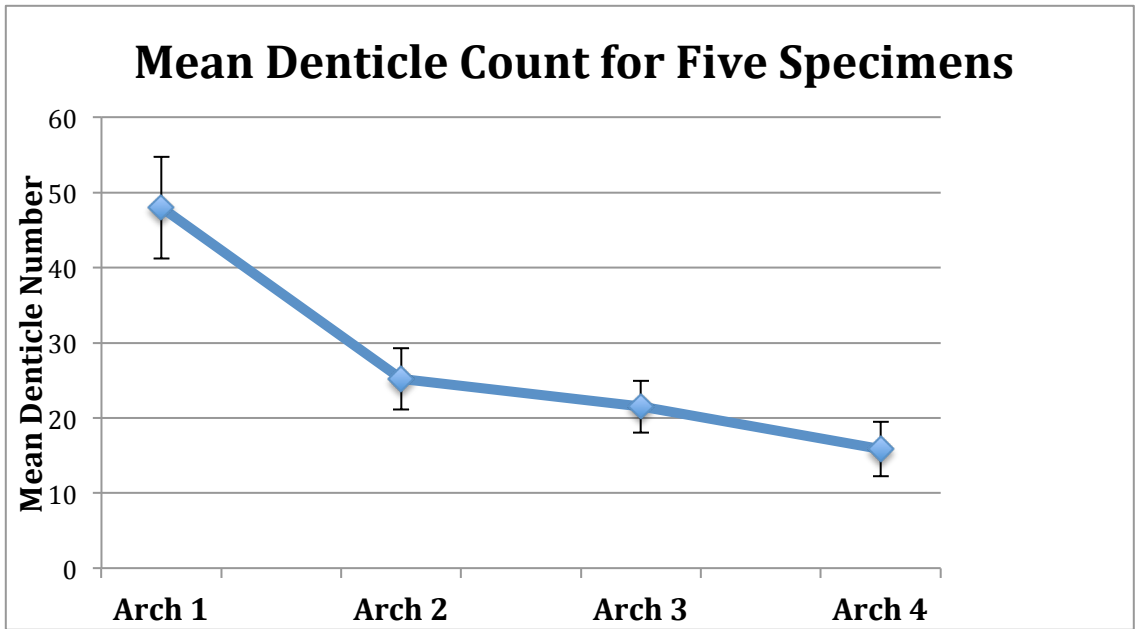


Figure 17: Graph with the mean value of total denticles along the raker from each of the five specimens. The mean value was calculated for each arch and the standard deviation is shown for each point.

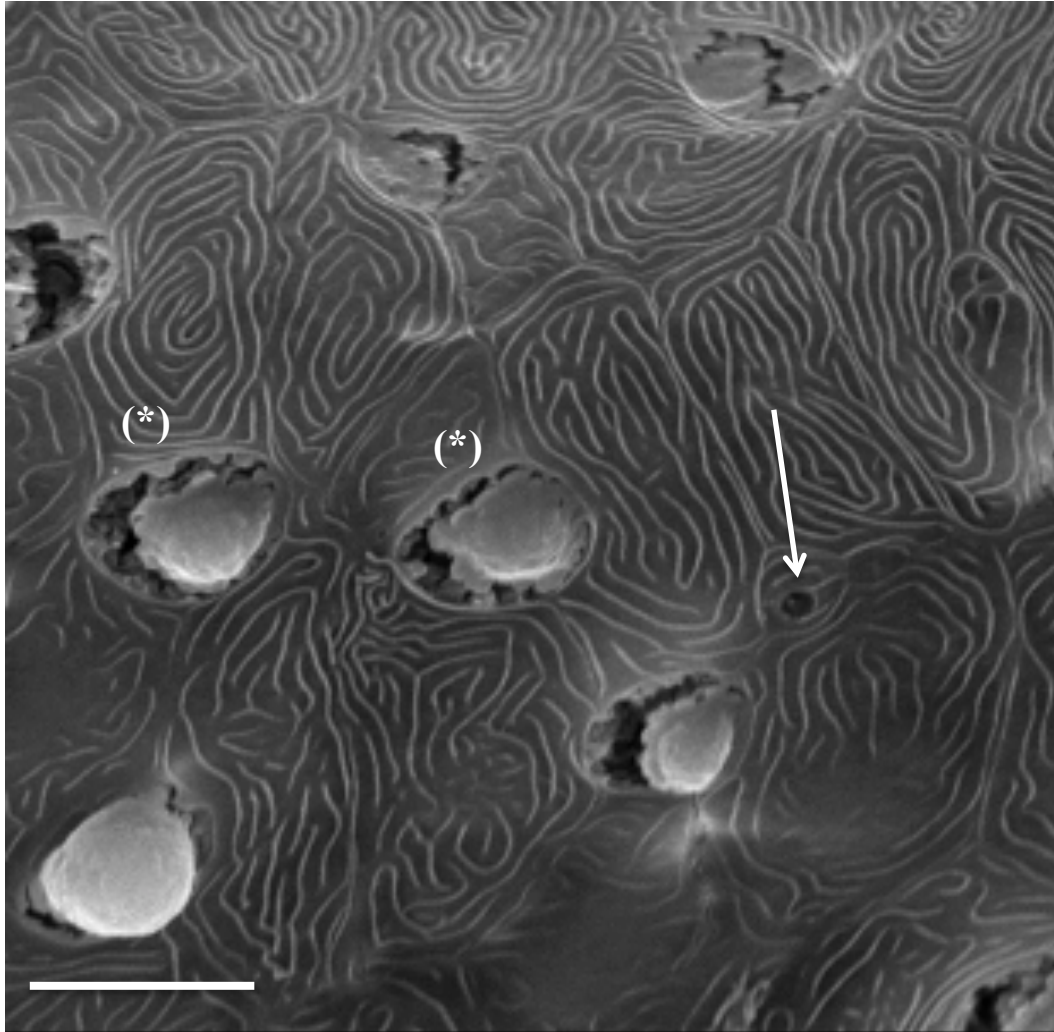


Figure 18: Surface chloride cell (arrow) shown next to mucous cells (*) on the gill raker. Scale bar 10 μm .